

Nonlinear amplifier and frequency shifter using a tunable periodic drive

Sergey Savel'ev,¹ A. L. Rakhmanov,^{1,2} and Franco Nori^{1,3}

¹Frontier Research System, The Institute of Physical and Chemical Research (RIKEN), Wako-shi, Saitama, 351-0198, Japan

²Institute for Theoretical and Applied Electrodynamics RAS, 125412 Moscow, Russia

³Center for Theoretical Physics, Department of Physics, University of Michigan, Ann Arbor, Michigan 48109-1120, USA

(Received 7 August 2004; revised manuscript received 1 August 2005; published 30 November 2005)

We consider the superposition of a weak and a strong force acting on an overdamped particle moving on either an asymmetric-periodic or a double-well potential. The velocity of the particle has only harmonics ($n\omega_1$) of the strong force, when the particle either oscillates near a minimum or runs away from it. Near a threshold drive (bistable point) separating these two dynamical regimes, the weak force drastically changes the velocity spectrum, greatly amplifying the mixing harmonics. This effect can be used either to amplify or to shift the frequency of a weak signal and can be observed in a wide variety of systems, including domain walls in a ferromagnet, SQUIDS, and tiny particles in a ratchet potential.

DOI: 10.1103/PhysRevE.72.056136

PACS number(s): 05.60.Cd

I. INTRODUCTION

Amplification of a weak signal is an important process in many physical and biophysical systems, as well as for applications (see, e.g., Ref. [1]). In mechanical and electrical devices, an amplified response can be achieved by using linear or nonlinear resonances, e.g., resonances in oscillating electrical circuits. Alternative mechanisms of signal amplification and frequency-shift control are of general physical interest since these might be more effective and convenient for particular applications.

A recently studied amplification principle is the well-known stochastic resonance (SR) [2], utilizing noise to amplify a weak signal. This effect was successfully used for understanding several phenomena in physical, biological, and even geological systems, including bistable lasers, semiconductor devices, chemical reactions, mechanoreceptor cells, etc [2]. Even though this effect has been used for the amplification of signals in some amplifiers, SR is rather limited in controllability since it has only one adjusting parameter, the noise strength. In order to achieve a better control of the signal amplification, Ref. [3] suggested to manipulate SR via two periodic signals with commensurate frequencies and turning the noise strength to a certain value.

Summary of this work: Here, we present an alternative deterministic (in contrast to stochastic resonance [2,3] and diffusion amplification [4]) method of signal amplification in nonlinear devices by applying an additional periodic driving with rather large amplitude with respect to a weak drive. By mixing these two signals we can sufficiently amplify the weak one and shift its frequency to a desirable range. This effect exhibits a threshold behavior and occurs if the strong drive brings the system close to a bistable point. As an example of this amplification mechanism, we consider the motion of an overdamped particle in either a ratchet [5] or a double-well potential [2].

As a possible experimental realization of the general effect proposed here, we discuss two examples, the motion of a domain wall in a patterned magnetic film, and also the amplification of a signal (ac current or ac field) in an asymmetric SQUID [6]. Note that the mechanism presented here explains the huge amplification (by a factor of 10^5) of radio

signals in amorphous magnetic ribbons, recently reported in Ref. [7].

A brief summary of the general result follows: Consider a strong drive ($A \cos \Omega_1 t$) and a weak signal ($\varepsilon \cos \Omega_2 t$, $\varepsilon \ll A$) which are the inputs to the nonlinear device described below. In Fourier space, the response of this device has two parts, their separate responses and mixing.

(1) The separate responses of two signals (without mixing) are

$$\mathcal{A}(\Omega) = A \hat{\mathcal{A}}(\Omega) \delta(\Omega, n\Omega_1) \quad (1)$$

and

$$\mathcal{E}(\Omega) = \varepsilon \hat{\mathcal{E}}(\Omega) \delta(\Omega, m\Omega_2). \quad (2)$$

These are just the harmonics of the two inputs. Here,

$$\hat{\mathcal{A}}(n\Omega_1) \sim \hat{\mathcal{E}}(m\Omega_2) \sim 1 \quad (3)$$

for the main peaks ($m, n=1$ or 2 and decreasing for increasing m, n), δ is the Kronecker symbol [e.g., $\delta(\Omega, n\Omega_1)=1$ when $\Omega=n\Omega_1$, and zero otherwise].

(2) When mixing occurs, the (amplified) response becomes

$$M(\Omega) = \hat{M}(A, \varepsilon; \Omega) \delta(\Omega, n\Omega_1 + m\Omega_2), \quad (4)$$

with

$$\varepsilon \ll \hat{M}(\varepsilon) \lesssim A \hat{\mathcal{A}} \quad (5)$$

(i.e., the output \hat{M} of the initially weak signal is now almost as large as the strong drive) if the drive brings the system near the bistable point; otherwise the response is not amplified and

$$\hat{M} \sim \varepsilon. \quad (6)$$

If $\varepsilon(t)$ is a slow function of time [i.e., $(\dot{\varepsilon}/\varepsilon) \ll \omega_1, \omega_2$ and the dot denotes a time derivative: $\equiv d/dt$], then in this case the proposed mechanism can be used to amplify the original signal $\varepsilon(t)$. This is our amplitude modulation (AM) amplifier,

$$M[\varepsilon(t)] \gg \varepsilon(t). \quad (7)$$

This mechanism can also be used to shift the spectral weight of the output to a desired range, including very low frequencies (compared to Ω_1, Ω_2). This can act like a frequency modulator (FM) or frequency shifter. Thus, we found a quite nontrivial effect of signal amplification in Fourier space, though there is no obvious signal amplification in the time domain.

This paper is organized as follows: the model used is described in Sec. II; the amplification of a weak signal, as well as the influence of noise, are discussed in Sec. III; and Sec. IV describes several examples of physical systems where the predicted phenomenon can be observed.

II. MODEL

Just as an illustrative example, let us consider the motion of an overdamped particle described by a coordinate x in a nonlinear potential well $U(x)$. The motion of this particle is driven by an external periodic driving force $A \cos \Omega_1 t$ and a weak periodic signal $\varepsilon \cos \Omega_2 t$ ($\varepsilon \ll A$). Using dimensionless variables $y=x/x_0$ and $\tau=t/t_0$ the corresponding dynamic equation reads

$$\dot{y} = -\frac{\partial u}{\partial y} + a \cos \omega_1 \tau + \varepsilon \cos \omega_2 \tau, \quad (8)$$

where

$$\begin{aligned} u &= U/U_0, & a &= Ax_0/U_0, \\ \varepsilon &= \varepsilon x_0/U_0, & \omega_{1,2} &= \Omega_{1,2} t_0. \end{aligned} \quad (9)$$

Here, U_0 and x_0 are the characteristic potential well height and spatial scale, and the characteristic time is chosen as $t_0 = x_0^2 \beta / U_0$; β is a damping parameter. We perform a simulation of Eq. (8) for two cases, the ratchet-type potential shown in Fig. 1(a), and a double-well potential, Fig. 1(b). We numerically obtain the particle coordinate $y(\tau)$ and the velocity $\dot{y}(\tau)$ and then calculate the Fourier transform, $\dot{y}(\omega)$, of $\dot{y}(\tau)$. Note that the output, $\dot{y}(\omega)$, can be directly measured in experiments; for instance, by measuring the voltage through a SQUID (using a lock-in amplifier).

III. AMPLIFICATION OF WEAK SIGNAL

A. Amplification at zero noise

We start our discussion by considering a ratchet potential [5]. Physical implementations of ratchet devices appear in Ref. [8]. When slowly increasing the amplitude of the ac driving force, we observe that the confined motion of the particle near a potential minimum is eventually changed to a directed (rectified) motion. When the driving force sufficiently exceeds a rectification threshold, called here bistable point, the typical Fourier transform $\dot{y}(\omega)$ [Fig. 2(a)] exhibits a set of peaks corresponding to the driving frequency ω_1 and its harmonics $n\omega_1$, where n is an integer. Harmonics, $n \neq 1$, occur due to the nonlinearity of the potential. The output $\dot{y}(\omega)$ is practically independent of the presence or absence of

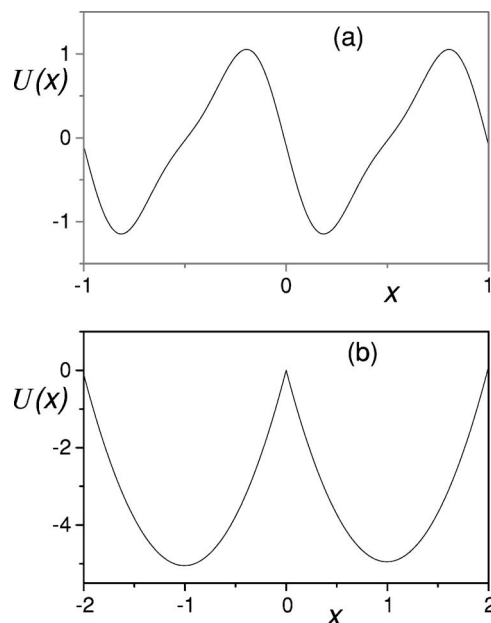


FIG. 1. Spatially asymmetric ratchet (a) and double-well (b) potentials used here to obtain the amplification of a weak signal. A particle moving in these potentials exhibits bistable dynamics, needed for the signal amplification studied here.

a small additional force $\varepsilon \cos \omega_2 \tau$, this signal is too weak to affect the motion of the particle.

The picture drastically changes within a narrow window of driving amplitudes and frequencies near the rectification threshold, from the nonamplified response shown, e.g., by the arrow in Fig. 2(a) to the amplified output \hat{M} in Figs. 2(b) and 2(c). Thus, near the bistable point, many additional peaks in $\dot{y}(\omega)$ appear. The additional peaks correspond to the combinations $n\omega_1 + m\omega_2$, where n, m are integers (either negative or positive). The heights of the peaks slowly decrease with increasing n, m and for the first several peaks are of the order of the main peak, corresponding to ω_1 .

In strong contrast to the mixing signal reported in Refs. [9,10] and the two-signal SR [3], both of which only occur for commensurate ω_1 and ω_2 and are controlled by the relative phases of two applied signals, this amplification (discussed here) of the weak signal occurs for both commensurate and incommensurate drives. Also, the spectrum $\dot{y}(\omega)$ studied here exhibits different properties for commensurate ($\omega_1/\omega_2 = p/q$) and incommensurate ($\omega_1/\omega_2 \neq p/q$) input frequencies with integer p and q [Figs. 2(b) and 2(c)]. Namely, a series of well separated peaks with relatively large amplitudes appear for commensurate frequencies, otherwise a dense set of smaller peaks occurs in addition to the large peaks in \hat{M} .

This unusual amplification

$$\hat{M}(a, \varepsilon) \sim a \hat{A} \quad (10)$$

is observed within a few percent of the driving amplitude a or frequency ω_1 . Note that such a tuning of the input amplitude a and frequency ω_1 can be easily achieved in experiments.

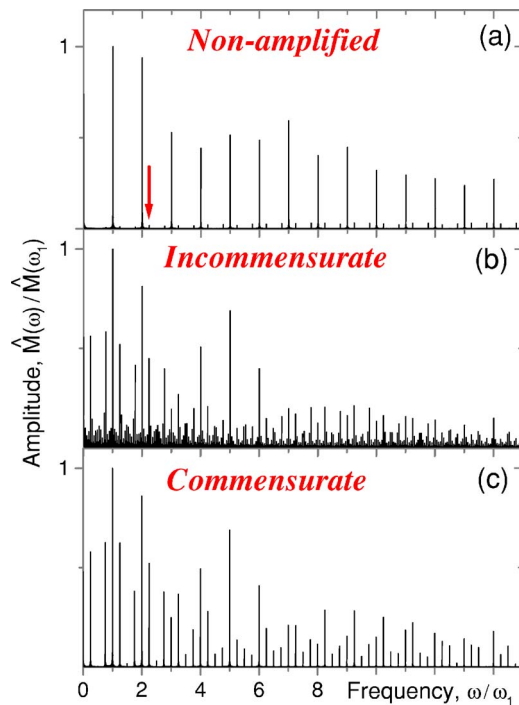


FIG. 2. (Color online) (a) The Fourier spectrum of the velocity of a particle in a ratchet potential, shown in Fig. 1(a), for the driving amplitude $a=7$, which is away from the bistable point, the response is given by the strong drive and its harmonics (the weak signal plays no role here). (b) Same as in (a) but with $a=6.72$ (which is close to a bistable point between confined and running solutions) and frequency $\omega_1=2\pi$. The weak signal amplitude is chosen to be $\epsilon=0.03$ and $\omega_2=\sqrt{5}\omega_1$. It is remarkable that even though the weak signal is $\leq 0.5\%$ of the strong force, the produced harmonic amplitudes are of the same order as the main drive. (c) Same as in (a) for commensurate frequencies, $\omega_2=(9/5)\omega_1=2.25\omega_1$ and $a=6.72$, i.e., close to the bistable point. Even though the weak signal frequency $\omega_2=(9/4)\omega_1$ is close to the incommensurate frequency in (b), the dense set of weak peaks disappears for the commensurate case (c). The labels (“Incommensurate”) “Commensurate” in the figures refer to the (in)commensurate ratio ω_2/ω_1 . The incommensurate case has fractal spectral structure.

It is important to stress that the effect discussed here is not related to the spatial asymmetry of the ratchet potential. Indeed, the same effect is revealed for the symmetric double-well potential in Fig. 3. A set of high amplitude harmonics $n\omega_1+m\omega_2$, for commensurate and incommensurate frequencies, emerges only near the threshold values of a and ω_1 when the particle starts to overcome the potential barrier and moves back and forth from one minimum to another. Thus, the amplification occurs near the bistable point similar to the studied above case of a particle moving in a ratchet potential. Nevertheless, the motion of the particle is different for double-well and ratchet potentials. For the former case the particle is trapped within a potential minimum at weak driving and quasiperiodically oscillates [see Fig. 4(b)] between two minima near the bistable point when the discussed amplification occurs. For the motion on a ratchet potential, the particle is localized near a minima for weak forces and starts to travel in a natural ratchet direction jumping [Fig. 4(a)]

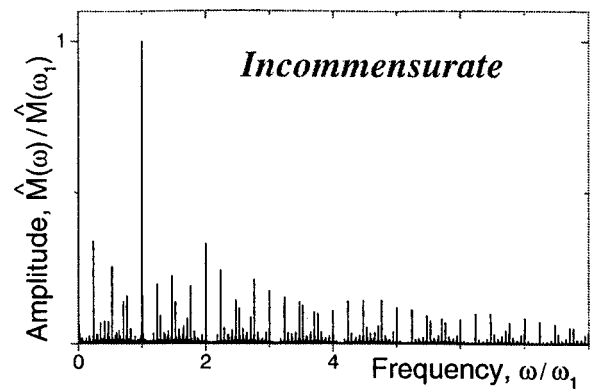


FIG. 3. The Fourier spectrum of the velocity of a particle in a double-well potential [shown in Fig. 1(b)] with frequencies as in Fig. 2(b) and $a=11.8, \epsilon=0.4$. In order to achieve amplification of a weak signal, the driving amplitude a is chosen to be close to the bistable point [located between the regions (i) where the particle motion is confined within one well, and (ii) where the motion occurs between the wells].

from time to time from one minimum to the next one, resulting in a net particle current.

The harmonic amplitudes

$$\hat{M}_{n,m} \equiv \hat{M}(n\omega_1 + m\omega_2) \quad (11)$$

of the response of the particle depend on the weak signal amplitude ϵ . As an illustration, the dependence of the amplitude

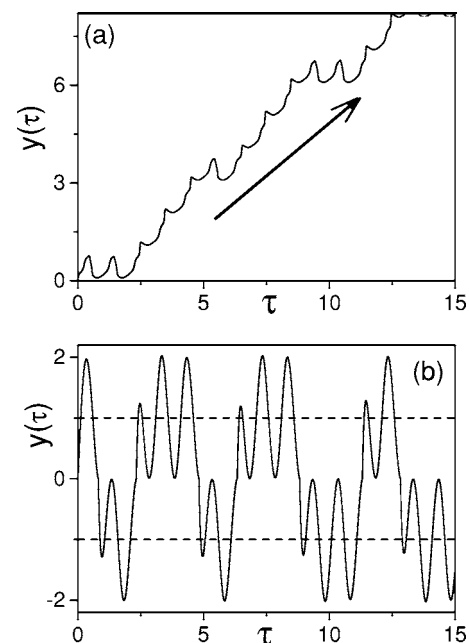


FIG. 4. The motion of the particle, on the ratchet potential [Fig. 1(a)] and the double-well potential [Fig. 1(b)], is shown in (a) and (b), respectively, for the parameters used in Fig. 2(b) and Fig. 3. The running solution $y(\tau)$ for the particle on the ratchet produces a net transport (shown by the arrow). The particle in the double-well potential jumps in (b) between two potential wells.

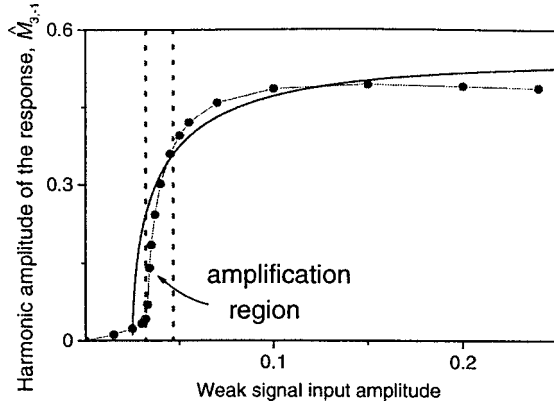


FIG. 5. Amplified harmonic $\hat{M}_{3,-1}(\epsilon) = \hat{M}(3\omega_1 - \omega_2)$ of the response $\hat{M}(\omega)$ versus the amplitude ϵ of a weak input signal for $a=6.72$ (near bistable point), $\omega_1 = \omega_2/\sqrt{5} = 2\pi$, for the ratchet potential shown in Fig. 1(a). Circles correspond to numerical results and the solid line is a fit using our derived result $\hat{M}_{n,m}(\epsilon) = \alpha \arccos[(a_c - a)/\epsilon]$, here with $a - a_c = 0.025$ and $\alpha = 0.36$. The region for the effective amplification of the weak signal is located between the two dashed lines.

$$\hat{M}_{3,-1} = \hat{M}(3\omega_1 - \omega_2) \quad (12)$$

on ϵ is shown in Fig. 5 for the ratchet potential [Fig. 1(a)]. The dependence is strongly nonlinear, first, $\hat{M}_{3,-1}(\epsilon)$ slightly grows for small ϵ ; then it sharply increases and finally it saturates. In general we can tune the output signal amplitude by changing either the height of the potential well or both the amplitude a and the frequency ω_1 of the driving force. In principle, under an appropriate choice of a and ω_1 the amplification factor $\hat{M}(\epsilon)/\epsilon$ [i.e., the ratio of the amplified harmonic $\hat{M}(\epsilon)$ to the amplitude ϵ of the weak signal] could be as large as $\sim a/\epsilon \gg 1$.

B. Analytical approach

The physical nature of this deterministic amplification mechanism has some common features with stochastic resonance. At low driving amplitudes the particle moves near one of the potential well minima. With increasing a , it approaches the potential maximum. If the weak signal amplitude is sufficient to assist the particle to overcome the barrier, then a series of additional harmonics arises in the Fourier spectrum $\dot{y}(\omega)$. Note that we have observed the same effect if the driving amplitude slightly exceeds the critical value $a_c(\omega_1)$. Thus, the criterion of amplification at a fixed driving frequency ω_1 is

$$\epsilon \leq |a_c(\omega_1) - a|, \quad (13)$$

where $a_c(\omega_1)$ is the driving amplitude necessary to overcome the barrier. If the driving force is significantly higher than the threshold value, the particle regularly passes over the potential barrier and the effect of the weak signal becomes negligible.

If the frequencies $\omega_{1,2}$ are commensurate, $\omega_1/\omega_2 = p/q$, then the sum of the strong and weak forces has a common

period $T = 2\pi p/\omega_1 = 2\pi q/\omega_2$. The peaks of the spectra $\dot{y}(\omega)$ shown in Fig. 2(c) correspond to such common period. If the frequencies are incommensurate, the sum of the strong and the weak input forces is not a periodic function and the output has a dense set of harmonics (corresponding to quasiperiodic motion). The highest harmonic is one of the closest combinations $n\omega_1 + m\omega_2$ to ω_1 .

Now we can better understand the dependence of the harmonic $\hat{M}_{n,m}$ on the weak input signal amplitude, Fig. 5. At low drive, this amplitude corresponds to the nonamplified output. If a approaches a_c , the weak input signal causes particle jumps over the barrier, and the number of such jumps increases with the amplitude ϵ and $\hat{M}_{n,m}(\epsilon)$ grows sharply. The number of these induced transitions saturates at higher ϵ , resulting in the saturation of the curve $\hat{M}_{n,m}(\epsilon)$. For low values of ω_1 and ω_2 , the weak signal $\epsilon \cos \omega_2 t$ does not vary significantly when the particle is in a narrow region near the unstable point. Thus, the particle overcomes a barrier, at $\tau = \tau_i$, if $\epsilon \cos \omega_2 \tau_i$ is larger than $|a_c(\omega_1) - a|$. Following Ref. [9], we assume that the times τ_i are distributed uniformly and the harmonic amplitude is proportional to the number of transitions over the barrier stimulated by the weak input signal. In this case we obtain the estimate

$$\hat{M}_{n,m}(\epsilon) \propto \arccos[(a_c - a)/\epsilon]. \quad (14)$$

This dependence is reasonably close to the numerical results (Fig. 5). Our analysis shows that the threshold amplitude a_c increases with ω_1 . Therefore, the amplification is suppressed at high frequencies, $\omega_1 \gg 1$, since the pumping energy becomes much higher than the potential barrier.

C. Gradual suppression of signal amplification by noise

The problem of noise is of importance for us since the nonlinear devices discussed here can also amplify undesirable noise. We simulate the effect of white noise on the amplification of the weak signal. Thus now we add a random force $\xi(\tau)$ to Eq. (8); with vanishing mean value $\langle \xi(\tau) \rangle = 0$ and correlation function $\langle \xi(\tau)\xi(0) \rangle = \kappa\delta(\tau)$. If the noise is realized by coupling to a heat bath with temperature T then, in our dimensionless variables, the strength of the noise is $\kappa = 2k_B T/U_0$. Numerical results for the ratchet potential are shown in Fig. 6 for different values of κ . Of course, relatively large noise eliminates the amplification effect. For lower κ , some fingerprints of the signal harmonics with highest amplitude could be resolved, Fig. 6(a). When decreasing the noise strength, more and more harmonics become visible, Fig. 6(b). As seen from Eq. (8), the contribution $\delta\dot{y}$ of the weak signal to the particle velocity is of the order of ϵ , while the mean square of the contribution of the noise to \dot{y} is evidently given by κ . Thus, a weak signal will be amplified if $\epsilon \gg \sqrt{\kappa}$, or in other words, if the weak signal energy ϵ^2 is higher than $k_B T$.

IV. TWO CANDIDATE PHYSICAL SYSTEMS TO OBSERVE SIGNAL AMPLIFICATION

As concrete examples of physical realizations of this proposed amplification process, we discuss

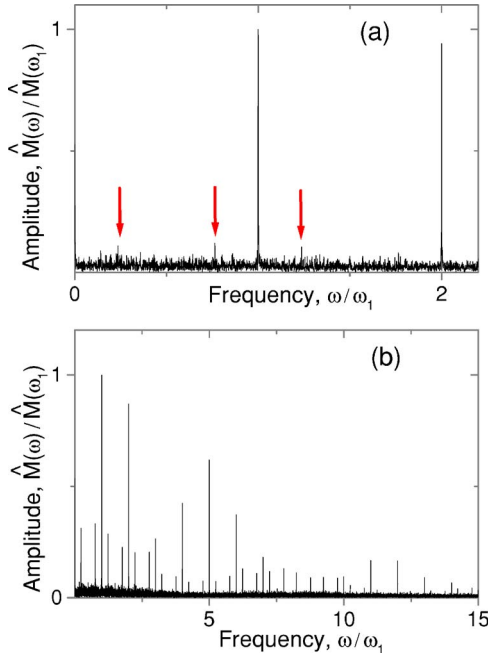


FIG. 6. (Color online) Gradual suppression of the amplified signal (particle velocity) by white noise for the ratchet potential shown in Fig. 1(a). Here, $a=6.72$, $\omega_1=\omega_2/\sqrt{5}=2\pi$, and $\epsilon=0.06$. For noise intensity $\kappa=10^{-3}$ [panel (a)], a weak trace of the input weak signal is barely visible (marked by red vertical arrows); for $\kappa=10^{-4}$ [panel (b)] the amplified peaks are well resolved.

- (1) a voltage signal in an asymmetric SQUID [Fig. 7(a)] with three junctions, and
- (2) domain wall motion in a ferromagnetic film [Fig. 7(b)].

Of course, this list is not exhaustive.

A. Asymmetric SQUID

In the overdamped limit, the equation for the total phase ϕ across the asymmetric SQUID [6] with three junctions is

$$\frac{\hbar c}{2eR} \dot{\phi} = -J_l \sin(\phi/2) - J_r \sin(\phi - \phi_{\text{ext}}) + I(t) + \xi(t), \quad (15)$$

where $R_l=R_r=R$ is the resistance of each junction, J_l and J_r are the critical currents, indexes l and r relate to the left and right branches of the SQUID [Fig. 7(a)]. This SQUID can be driven by a current having both strong and weak currents [Fig. 7(a)],

$$I(t) = I_0(\sin \Omega_1 t + \epsilon \sin \Omega_2 t). \quad (16)$$

The total voltage across the SQUID and the external magnetic flux in the ring are respectively, $V=\Phi_0 \dot{\phi}/c$ and $\Phi_{\text{ext}}=\phi_{\text{ext}}\Phi_0$, where Φ_0 is the flux quantum. We also assume Gaussian white noise. Using dimensionless variables, we obtain Eq. (8) with $t_0=\hbar/2eRJ_c$, $a=I_0/J_c$, $J_c=J_r+J_l$, and the dimensionless strength of the white noise is $\kappa=2k_B T \hbar/eRJ_c$. Using, e.g., $R\sim 0.1\Omega$, $J_c\sim 100\mu\text{A}$, we find that the characteristic frequencies are in the 1–10 GHz range. The weak

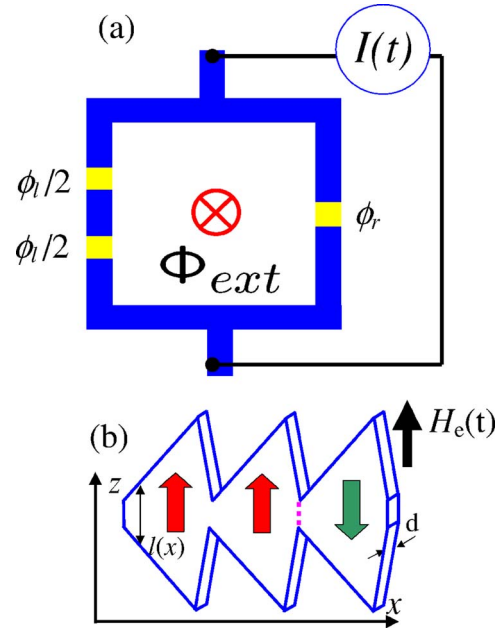


FIG. 7. (Color online) (a) A schematic view of the asymmetric SQUID with two Josephson junctions on the left branch (both of them described by the gauge-invariant phase $\phi_l \equiv \phi$) and one Josephson junction on the right branch (with phase ϕ_r). (b) 3D sketch of a triangular-patterned magnetic film, indicating the height $l(x)$ and width d . The magnetic domain-wall (shown by the short vertical dashed magenta line) separates regions having different orientations of the magnetization (shown by the up and down arrows). This wall can be driven through the patterned magnetic sample by applying a time-dependent external magnetic field $H_e(t)$.

current will be amplified if $\epsilon \geq \sqrt{0.05T(\text{K})/J_c(\mu\text{A})}$ or, at $T\sim 1\text{K}$, the weak input signal will be amplified if it exceeds $\sim 2\%$ of J_c . The characteristic value of the amplified voltage peaks will be about $1\mu\text{V}$. The same mechanism of amplification can be used for a weak magnetic flux through the SQUID loop. In principle, this allows to improve its sensitivity up to $\Phi_0 \epsilon \ll \Phi_0$. In other words, near a bistable point the sensitivity of a SQUID could be greatly enhanced, allowing it to detect very small ($\ll \Phi_0$) ac magnetic fluxes.

B. Magnetic domain wall

Under rather general assumptions, the motion of a domain wall in a ferromagnetic metal can be described in terms of the dynamics of an overdamped particle. Let us consider a ferromagnetic film patterned in the shape of either a periodic ratchet [Fig. 7(b)] or as a double well. The easy axis is inside the film plane and is pointed perpendicular to the x -axis. If the magnetic anisotropy field H_a is not very small, the magnetization vector will be parallel to the easy axis and domain walls would also be parallel to this axis. Neglecting stray magnetic fields, the energy of the film [driven by the external magnetic field $H_e(t)$ applied in the film plane and perpendicular to the x direction] can be written as

$$E(x) = E_W l(x)d - 2MH_e(t)d \int_0^x l(x')dx', \quad (17)$$

where E_W is the domain wall energy per unit area, $l(x)$ is the variable film width, d is the film thickness, and M is the

magnetization. The second term is the usual Zeeman energy. We assume that the external field is the sum of a driving force, $H_0 \cos \Omega_1 t$, and a weak signal, $\epsilon H_0 \cos \Omega_2 t$, i.e.,

$$H_e(t) = H_0 \cos \Omega_1 t + \epsilon H_0 \cos \Omega_2 t. \quad (18)$$

The friction force acting on the domain wall consists of two parts: a pinning force, $-f_p \dot{x}/|\dot{x}|$, and the eddy current contribution,

$$\text{“eddy friction”} = \beta \dot{x} l(x) d, \quad (19)$$

with

$$\beta = \gamma_1 (2\pi M)^2 d l \rho c^2 \quad (20)$$

(where ρ is the resistivity and γ_1 is a constant of the order of unity). Friction forces of this type appear in many systems (see, e.g., [11] for studies of friction in mechanical, electric, and magnetic systems). Using $u(y) = \ln l(y)$, Eq. (8) can be derived from (17) with

$$a = 2H_0 M x_0 / E_W, \quad (21)$$

when adding an additional pinning force f_p/E_W . Our numerical and analytical studies reveal that the pinning force does not affect the spectrum $\dot{y}(\omega)$, besides shifting the threshold amplitude of the drive by f_p/E_W . The domain wall energy is

$$E_W = \gamma M^{3/2} H_a^{1/2} l_{\text{ex}}, \quad (22)$$

where γ is of the order of unity and l_{ex} is the exchange length. The film can be placed in a pick-up coil with the axis along the magnetization vector. Then, a voltage $V(t)$ proportional to \dot{x} will be induced in the coil. Using Faraday's law we find that the frequency spectrum of this voltage is

$$V(\omega) = 8\pi N M x_0 \dot{y}(\omega) d l c t_0, \quad (23)$$

where N is the number of turns in the coil. The ferromagnet amplifies the signal in the coil even if the weak signal alone

could be so weak that it cannot overcome the domain wall pinning. The applied additional drive allows to amplify this weak signal by orders of magnitude. Using $M \sim 1$ kOe, $H_a \sim 10$ Oe, $l_{\text{ex}} \sim 3$ nm, $x_0 \sim 1$ μ m, and $\rho \sim 1$ $\mu\Omega$ m, we find that ω_1 and ω_2 lie in the 10 kHz range and the stronger driving amplitude ~ 1 Oe. The voltage output due to the weak signal is ~ 10 nV per turn. The effect of the thermal noise on this device can be neglected even at room temperatures.

Note that the microscale magnetic ratchet discussed above can also be used as a step motor [12] to precisely control the motion of domain walls between discrete positions corresponding to the narrowest parts of the patterned [as in Fig. 7(b)] film. In order to shift the domain wall by n steps, we should apply a magnetic field pulse with amplitude H_0 and duration Δt obeying the equation $H_0 \Delta t \approx n \cdot 2\pi^2 x_0 M d / c^2 \rho \approx 2 \times 10^{-9}$ Oe s for $H_0 \ll l_{\text{ex}} \sqrt{M H_a} / x_0 \approx 0.3$ Oe.

V. CONCLUSIONS

Near a bistable point, we propose a general mechanism for nonlinear amplification and shifting the output response to a desirable frequency. We illustrate this general effect with several examples, including asymmetric SQUIDS, particle motion, and domain wall motion in patterned ferromagnetic films.

ACKNOWLEDGMENTS

This work was supported in part by the National Security Agency (NSA) and Advanced Research and Development Activity (ARDA) under Air Force Office of Research (AFOSR) Contract No. F49620-02-1-0334; and also supported by the US National Science Foundation Grant No. EIA-0130383.

-
- [1] B. D. Gomperts, I. M. Kramer, and P. E. R. Tatham, *Signal Transduction* (Academic, London, 2002).
- [2] L. Gammaitoni, P. Hänggi, P. Jung, and F. Marchesoni, *Rev. Mod. Phys.* **70**, 223 (1998), T. Wellens, V. Shatokhin, and A. Buchleitner, *Rep. Prog. Phys.* **67**, 45 (2004).
- [3] L. Gammaitoni, M. Löcher, A. Bulsara, P. Hänggi, J. Neff, K. Wiesenfeld, W. Ditto, and M. E. Inchiosa, *Phys. Rev. Lett.* **82**, 4574 (1999).
- [4] P. Reimann, C. Van den Broeck, H. Linke, P. Hänggi, J. M. Rubi, and A. Pérez-Madrid, *Phys. Rev. Lett.* **87**, 010602 (2001).
- [5] P. Reimann, *Phys. Rep.* **361**, 57 (2002); R. D. Astumian, and P. Hänggi, *Phys. Today* **55**, 33 (2002); H. Linke, *Appl. Phys. A: Mater. Sci. Process.* **75**, 167 (2002), special issue on Brownian motors; P. Hänggi, F. Marchesoni, and F. Nori, *Ann. Phys.* **14**, 51 (2005).
- [6] I. Zapata, R. Bartussek, F. Sols, and P. Hänggi, *Phys. Rev. Lett.* **77**, 2292 (1996).
- [7] A. S. Antonov, N. A. Buznikov, M. M. Filatov, V. P. Goncharov, A. A. Rakhmanov, and A. L. Rakhmanov, *J. Magn. Magn. Mater.* **258**, 198 (2003).
- [8] J. F. Wambaugh, C. Reichhardt, C. J. Olson, F. Marchesoni, and F. Nori, *Phys. Rev. Lett.* **83**, 5106 (1999); C. J. Olson, C. Reichhardt, B. Janko, and F. Nori, *ibid.* **87**, 177002 (2001); B. Y. Zhu, F. Marchesoni, and F. Nori, *ibid.* **92**, 180602 (2004); S. Savel'ev, F. Marchesoni, and F. Nori, *ibid.* **91**, 010601 (2003); Y. Togawa *et al.*, *ibid.* **95**, 087002 (2005).; S. Savel'ev and F. Nori, *Nat. Mater.* **1**, 179 (2002); J. E. Villegas *et al.*, *Science* **302**, 1188 (2003); B. Y. Zhu, F. Marchesoni, V. V. Moshchalkov, and F. Nori, *Phys. Rev. B* **68**, 014514 (2003); *Physica C* **388**, 665 (2003); **404**, 260 (2004); R. Wördenweber, P. Dymashevski, and V. R. Misko, *Phys. Rev. B* **69**, 184504 (2004); S. Savel'ev, V. Misko, F. Marchesoni, and F. Nori, *ibid.* **71**, 214303 (2005).
- [9] S. Savel'ev, F. Marchesoni, P. Hänggi, and F. Nori, *Europhys. Lett.* **67**, 179 (2004); *Eur. Phys. J. B* **40**, 403 (2004); *Phys. Rev. E* **70**, 066109 (2004).
- [10] S. Savel'ev, F. Marchesoni, and F. Nori, *Phys. Rev. Lett.* **92**, 160602 (2004).
- [11] A. Maeda *et al.*, *Phys. Rev. Lett.* **94**, 077001 (2005).
- [12] S. Savel'ev, A. Rakhmanov, and F. Nori, *New J. Phys.* **7**, 82 (2005).